

Ultrafast terahertz response in photoexcited, vertically grown few-layer graphene

Maixia Fu, Baogang Quan, Jingwen He, Zehan Yao, Changzhi Gu, Junjie Li, and Yan Zhang

Citation: [Applied Physics Letters](#) **108**, 121904 (2016); doi: 10.1063/1.4944887

View online: <http://dx.doi.org/10.1063/1.4944887>

View Table of Contents: <http://scitation.aip.org/content/aip/journal/apl/108/12?ver=pdfcov>

Published by the [AIP Publishing](#)

Articles you may be interested in

[Hot carrier and hot phonon coupling during ultrafast relaxation of photoexcited electrons in graphene](#)

Appl. Phys. Lett. **108**, 043105 (2016); 10.1063/1.4940902

[Ultrafast terahertz Faraday rotation in graphene](#)

J. Appl. Phys. **116**, 214302 (2014); 10.1063/1.4903212

[Observation of suppressed terahertz absorption in photoexcited graphene](#)

Appl. Phys. Lett. **102**, 113111 (2013); 10.1063/1.4795858

[Ultrafast carrier dynamics and saturable absorption of solution-processable few-layered graphene oxide](#)

Appl. Phys. Lett. **98**, 121905 (2011); 10.1063/1.3570640

[Broadband electromagnetic response and ultrafast dynamics of few-layer epitaxial graphene](#)

Appl. Phys. Lett. **94**, 172102 (2009); 10.1063/1.3122348

The advertisement features a blue background with a molecular structure of spheres and a bright light source. On the left, there is a thumbnail image of an 'Applied Physics Reviews' journal cover showing a layered material structure. The main text 'NEW Special Topic Sections' is in large white font. Below it, 'NOW ONLINE' is in yellow, followed by 'Lithium Niobate Properties and Applications: Reviews of Emerging Trends' in white. The AIP Applied Physics Reviews logo is in the bottom right corner.

NEW Special Topic Sections

NOW ONLINE
Lithium Niobate Properties and Applications:
Reviews of Emerging Trends

AIP Applied Physics
Reviews

Ultrafast terahertz response in photoexcited, vertically grown few-layer graphene

Maixia Fu,^{1,2} Baogang Quan,³ Jingwen He,¹ Zehan Yao,³ Changzhi Gu,³ Junjie Li,³ and Yan Zhang^{1,a)}

¹Beijing Key Laboratory for Metamaterials and Devices, and Key Laboratory of Terahertz Optoelectronics, Ministry of Education, Department of Physics, Capital Normal University, Beijing 100048, China

²College of Information Science and Engineering, Henan University of Technology, Zhengzhou, Henan 450001, China

³Beijing National Laboratory for Condensed Matter Physics, Institute of Physics, Chinese Academy of Sciences, Beijing 100190, China

(Received 18 December 2015; accepted 2 March 2016; published online 25 March 2016)

The terahertz (THz) response from vertically aligned few-layer graphene samples with and without femtosecond optical excitation was investigated. The frequency-dependent optical conductivity of the photoexcited vertically aligned few-layer graphene had a strong free carrier response. Upon photoexcitation, a transient decrease in THz transmission on the subpicosecond timescale was observed. A modulation depth of nearly 16% was demonstrated in the range of the photoexcitation power used. The photoinduced ultrafast response presented here is distinct from previous studies on horizontally grown graphene. The mechanism underlying this photoconductive ultrafast response was investigated by measuring the transmission properties and by calculating the carrier density. The results of these studies are promising for the development of high-performance THz modulators and ultrafast switchable THz photoelectric devices. © 2016 AIP Publishing LLC.

[<http://dx.doi.org/10.1063/1.4944887>]

Graphene is a gapless two-dimensional material with hexagonal lattice and linear electronic band dispersion for the electron and hole bands near the corners of the Brillouin zone. Graphene has attracted much attention for its exceptional physical properties,¹ such as the anomalous quantum Hall effect, extremely high carrier mobility, absorption that can saturate, and tunable interband and intraband conductivities.^{2–5} Thus far, experimental studies have confirmed that the interband transitions dominate in the infrared/visible range and give rise to a constant absorption of 2.3% by single-layer graphene at normal incidence.^{6–8} Intraband transitions dominate the terahertz (THz) range, resulting in a tunable optical conductivity that can be described using the Drude model.^{9,10} It is well known that graphene is one of the best materials for modulating the propagation properties of the THz wave. Many of the THz devices based on graphene have been reported.^{11,12} An important way to realize such modulation is to apply an external optical to graphene-related hybrid structures.¹³ Because of the intraband transitions or free carrier absorption,^{14,15} the Fermi level in graphene can be tuned and thus the optical conductivity can also be tuned. Recently, many studies of ultrafast optical pumping of graphene have been performed to investigate the evolution of the graphene optical response.^{16–19} This transient THz response is appealing, because it can directly mirror the dynamics of the free carriers without considering complex interband transitions. The response of carriers in nonequilibrium conditions is of particular importance for the generation of photocurrent in graphene, which can be used in photoelectric detectors and emitters.^{20,21} However, all of the reported research on graphene in the THz range concern

horizontally grown graphene. To date, the optical properties of vertically aligned few-layer graphene (VAFLG)^{22–24} in the THz range remain unexplored.

Recently, three-dimensional graphene has attracted much attention because of its high surface-area-to-volume ratio. The vertically aligned graphene nanosheet is a popular material with a three-dimensional carbon structure and has been used in various applications, such as field emitters,²⁵ supercapacitors,^{26–28} and batteries.²⁹ Therefore, the study of VAFLG will not only provide guidance for these applications, but also lay the foundation for and promote the development of relative applications in the THz range. In this paper, the VAFLG samples were measured using THz time domain spectroscopy and an optical pump system. A transient decrease of the THz transmission upon optical pumping was observed with a modulation depth of nearly 16%. The response time was on the subpicosecond scale. The graphene optical conductivity was fitted with the Drude model and agreed with the experimental results. According to the calculations and analysis, the increase of optical conductivity from the rise in carrier density is responsible for the observed phenomena. Owing to a transmission decrease with the increase in the pump power, the photoinduced ultrafast response presented here is clearly distinct from the previous reports of horizontally grown graphene on a quartz substrate. For horizontally grown few-layer graphene with a quartz substrate, the THz transmission increased with the rise in optical pump power,^{30,31} originate from the decrease of photoconductivity, the experimental modulation depth reported was just less than 5%, and the response time was on the picosecond scale. The research presented not only shows the diversity of responses in graphene depending on the method of sample growth, but more significantly demonstrates that

^{a)}yzhang@cnu.edu.cn

VAFLG can be applied in the development of ultrafast THz modulators and switchable THz devices.

The response of VAFLG was investigated with a time-resolved THz spectroscopy system. The experimental setup is schematically illustrated in Fig. 1(a). A femtosecond Ti:sapphire amplifier system with a repetition rate of 1 kHz and a central wavelength of 800 nm was used as the light source. The THz wave generated by a (110) ZnTe crystal was normally incident on the VAFLG. The THz wave and pump beam were all linearly polarized. The optical path of the pump beam and THz beam can be modulated with two electronically controlled moving stages. After passing the sample, the THz wave was collected with parabolic mirrors and measured with a differential detection setup. The VAFLG samples investigated in this study were prepared by microwave plasma-enhanced chemical vapor deposition. Figure 1(b) shows a scanning electron microscopy image of a VAFLG sample. The porosity of the VAFLG film is approximately

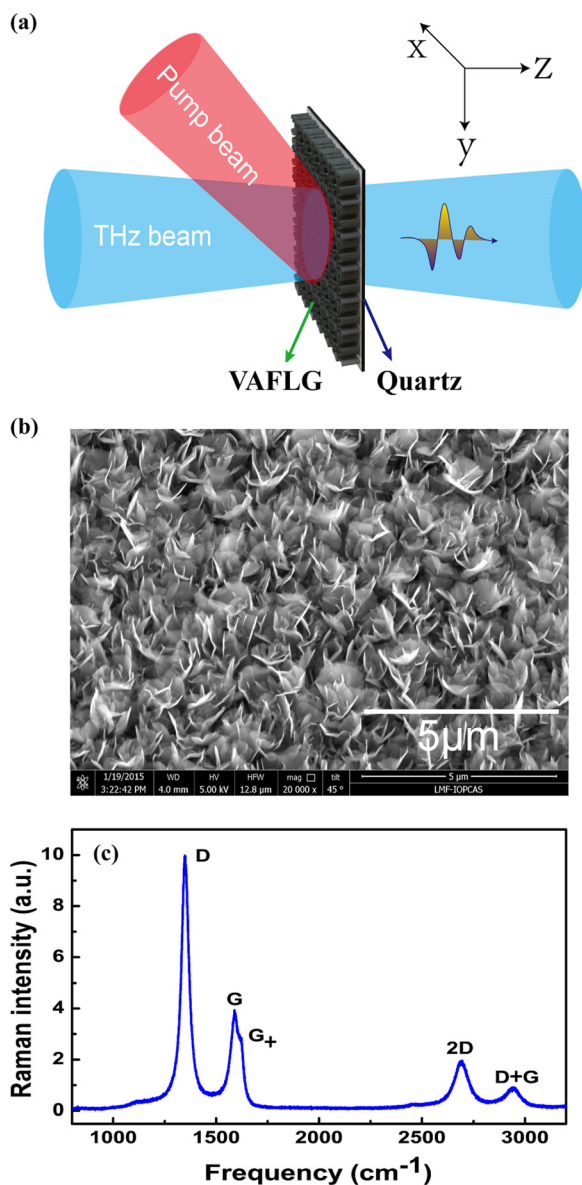


FIG. 1. (a) Schematic of the experimental setup. (b) Scanning electron microscopy image of the VAFLG sample. (c) Raman spectrum of VAFLG sample.

30%, and the sheet resistance is about $147 \Omega/\square$ employing a four-point probe technology. The thicknesses of the VAFLG film and quartz substrate are $1.8 \mu\text{m}$ and $500 \mu\text{m}$, respectively. Figure 1(c) describes a Raman spectrum of a VAFLG sample, providing useful information about the defects (D peak $\sim 1349 \text{ cm}^{-1}$), in-plane vibration of sp² carbon atoms (G peak $\sim 1589 \text{ cm}^{-1}$), as well as the stacking order (2D peak $\sim 2695 \text{ cm}^{-1}$). There is a split peak labeled G⁺ at 1621 cm^{-1} , which is due to in-plane vibrations along the vertically grown axis. The full-width at half-height maximum (FWHM) of 2D band is 80 cm^{-1} , and the intensity ratio of G/2D is about 2. Thus, the number of layers for VAFLG film is estimated to be between 5 and 10 (less than 10).

The transmission of the VAFLG sample was first measured without photoexcitation. The THz waves transmitted through the VAFLG sample and the bare quartz substrate are $E(t)$ and $E_0(t)$ as shown in Fig. 2(a). $E(\omega)$ and $E_0(\omega)$ are the corresponding spectra in the frequency domain. The amplitudes of $|E(\omega)|$ and $|E_0(\omega)|$ are shown in the inset of Fig. 2(a). A significant attenuation of THz transmission was observed, which arises from the strong response of charge carriers in the VAFLG sample. Considering that both the thickness and the pores' size of the VAFLG film are far smaller than the center wavelength of the THz wave used ($400 \mu\text{m}$), it is appropriate to apply thin-film approximation and an effective medium model to describe the experimental data.³² Therefore, the frequency-dependent equivalent complex conductivity $\tilde{\sigma}(\omega)$ of the VAFLG sample can be extracted from the measured transmission spectra using the following formula:³²

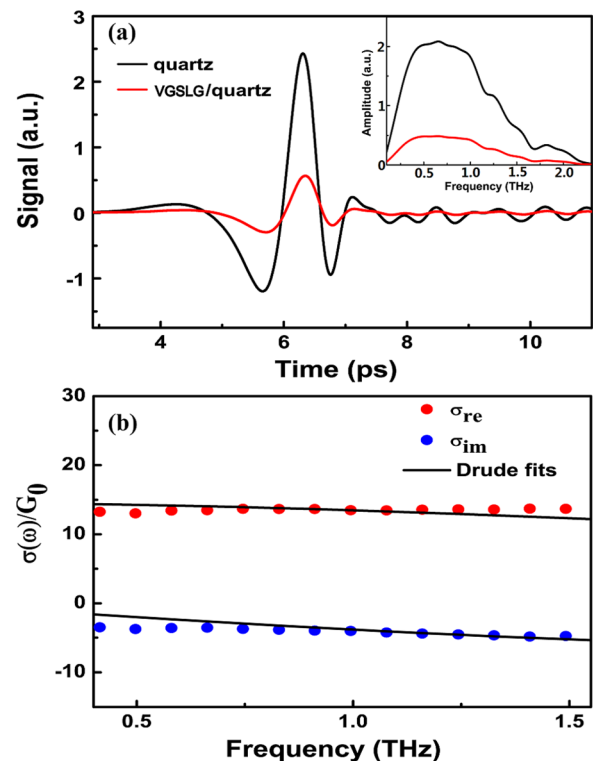


FIG. 2. (a) Measured THz waveforms transmitted through the VAFLG sample (red) and bare quartz substrate (black). The inset shows the corresponding frequency domain signals. (b) Experimental (dotted) and fitted (solid) complex conductivity of the VAFLG sample.

$$\frac{E(\omega)}{E_0(\omega)} = \frac{n_s + 1}{n_s + 1 + dZ_0\tilde{\sigma}(\omega)}, \quad (1)$$

where $n_s = 1.96$ is the refractive index of the quartz substrate, $Z_0 = 377 \Omega$ is the impedance of free space, ω is the angular frequency of the incident light, and $d = 1.8 \mu\text{m}$ is the thickness of the VAFLG sample. The complex conductivity of VAFLG is normalized by the quantum of conductance $G_0 = 2e^2/h$, where e is the electron charge and h is the Planck constant. Figure 2(b) illustrates the measured complex conductivity $\tilde{\sigma}(\omega)$ (dotted) of VAFLG. The real part of $\tilde{\sigma}(\omega)$ is nearly $14G_0$. This is large because of the high carrier density arising from the sample growth process combined with the relatively high carrier mobility. Note that the real part of the conductivity is almost constant for a particular THz frequency, indicating that the scattering rate of VAFLG is too high to observe any frequency dependence of the conductivity over the measured THz spectral range.^{33,34}

To fully understand the phenomenon observed, the experimental conductivity of a VAFLG sample was fitted with the Drude model:^{30–36}

$$\tilde{\sigma}(\omega) = \frac{iD}{\pi(\omega + i\Gamma)}, \quad (2)$$

where Γ is the average scattering rate of carriers and D is the Drude weight related to the density of carriers. The carrier density N is^{30–36}

$$N = \frac{\hbar^2}{\pi V_F^2 e^4} D^2, \quad (3)$$

where V_F is the Fermi velocity with a value of $1.1 \times 10^6 \text{ m/s}$ and \hbar is the reduced Planck constant. The solid lines in Fig. 2(b) are the Drude fitting results of the complex conductivity with a Drude weight of $D = 2.65 \times 10^3 G_0 \text{ cm}^{-1}$ and a carrier scattering rate of $\Gamma = 95.47 \text{ cm}^{-1}$. The results fit well with the experimental values in the measured spectral range. The density of carriers was $N = 1.66 \times 10^{10} / \text{cm}^2$, showing a strong response to the electric field. This is the origin of the attenuation of THz transmission.

The response of the VAFLG sample under external optical excitation was investigated using an optically pumped THz probe system. The power of the pumping beam was modulated with an attenuator. The THz wave had a delay time with respect to the pump beam to ensure that the VAFLG sample was excited when the THz wave arrived. The transmitted THz signal decreased when the photoexcited power increased from $0 \mu\text{J}/\text{cm}^2$ to $240 \mu\text{J}/\text{cm}^2$ as shown in Fig. 3(a). The phenomena observed here are clearly distinct from the reported phenomena for horizontally grown graphene on a quartz substrate, which showed a transmission increase with the increase in the pump power.³¹ The inset of Fig. 3(a) shows a magnified view of the peaks, which more clearly shows a pump-induced decrease of the THz transmission. For all experimental pump powers, the complex conductivity was calculated and fitted with the Drude model. The density of carriers under different pump powers was obtained according to Eq. (3). The modulation depth, M , is defined as $M = |E_p(\omega) - E(\omega)|/E(\omega)$, where $E_p(\omega)$ and

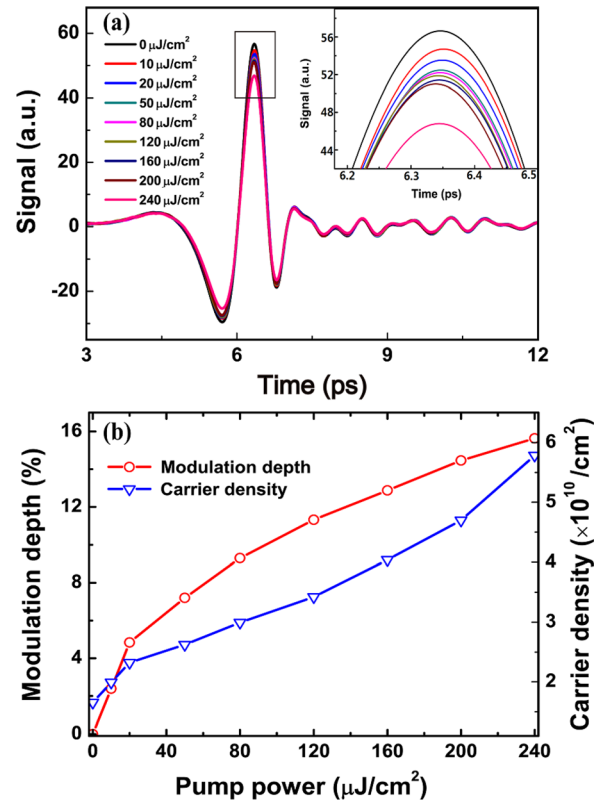


FIG. 3. (a) Transmitted THz signals of the VAFLG sample under different photoexcitation powers. The inset shows a magnified view of the peaks. (b) Dependence of the modulation depth and carrier density on photoexcited power.

$E(\omega)$ are the Fourier transforms of the transmitted THz signal with and without the optical pump, respectively. The dependence of the modulation depth, M , and carrier density, N , on the pump power was calculated and shown in Fig. 3(b). A modulation depth of nearly 16% was obtained with a pump power of $240 \mu\text{J}/\text{cm}^2$. The carrier density increased from $N = 1.66 \times 10^{10} / \text{cm}^2$ without optical excitation to $N = 5.78 \times 10^{10} / \text{cm}^2$ with the $240 \mu\text{J}/\text{cm}^2$ pump. It is obvious that the density of carriers increased with increasing pump power, leading to the rise in optical conductivity and consequently the decrease in THz transmission as shown in Fig. 3(a).

To further investigate the dynamic process of the optical response of the VAFLG sample, the moving stage controlling the optical path of the THz wave was fixed at the maximum of the THz signals, while the moving stage controlling the pump beam was scanned to modulate the time delay, τ , between the pump beam and THz wave. The time delay $\tau = 0$ means that the optical path of the THz wave and pump beam is equal, while $\tau < 0$ and $\tau > 0$ mean that the pump beam arrives at the VAFLG sample later or earlier than THz wave. The transmitted THz signals at different τ with different pump powers were recorded and given in Fig. 4(a). The photoinduced change in the maximum of the transmitted THz wave was normalized to the maximum of the THz wave without photoexcitation. The transmitted THz electric field decreased rapidly after photoexcitation on the subpicosecond time scale and then recovered to nearly the original value for all measured photoexcitation

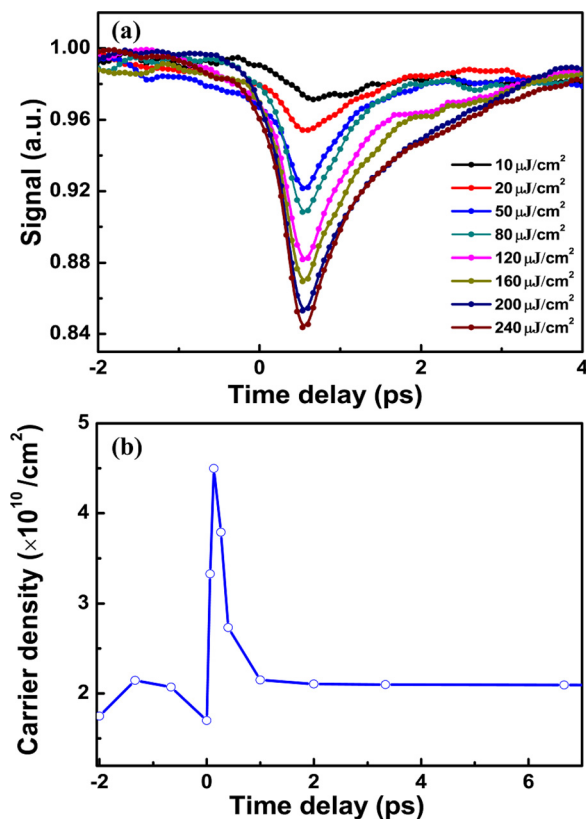


FIG. 4. (a) Changes in the maxima of the THz waveforms with photoexcitation at different time delays. The experiment data were normalized to the maxima of the THz waveforms without photoexcitation. (b) Evolution of the carrier density with different time delays under a pump power of $200 \mu\text{J}/\text{cm}^2$.

powers. Providing that the pump power is $240 \mu\text{J}/\text{cm}^2$, the transmitted THz electric field can transiently drop to 84% in less than half a picosecond. The observed phenomenon indicates that the stronger the power of the pump beam, the greater the transmitted THz electric field will fall. Therefore, a lower transmitted THz electric field can be obtained with a stronger pump power. These results are exciting for promising applications in THz technology, such as the development of high-performance THz modulators and ultrafast switchable THz optoelectronic devices.

The mechanism underlying this photoconductive ultrafast response was investigated by measuring the THz transmission properties at different time delays, τ , and by calculating the density of carriers. The pump power was set at a specific value, and the stage controlling the optical path of the pump beam was fixed at different τ . For each τ , the transmitted THz waves were recorded and analyzed. According to Eqs. (1), (2), and (3), the complex conductivity with its own Drude weight, D , and scattering rate, Γ , for each τ was calculated. The dependence of the carrier density on different τ with the pump power of $200 \mu\text{J}/\text{cm}^2$ was illustrated in Fig. 4(b). Upon photoexcitation, the density of carriers rises sharply from $N = 2.07 \times 10^{10}/\text{cm}^2$ for $\tau = -0.5$ ps to $N = 4.50 \times 10^{10}/\text{cm}^2$ for $\tau = 0.4$ ps. After photoexcitation, the density of carriers recovers to a value close to the original state. For a time delay of $\tau < 0$, the THz transmission obtained is equivalent to the state without photoexcitation. For $\tau > 0$, the optically generated carriers emerge when the THz wave arrives. The increase in N leads to the rise in the optical

conductivity and consequently to the decrease in THz transmission. Because graphene has an extremely high carrier mobility, the photogenerated carriers recombined as the time delay deviated from $\tau = 0$. The decrease in N leads to decline in optical conductivity, and therefore, the THz transmission returned to the initial state.

In conclusion, the THz response of VAFLG with and without a femtosecond optical pump was measured and analyzed. The frequency-dependent conductivity of the photoexcited VAFLG had a strong free carrier response. Upon photoexcitation, a transient decrease in THz transmission on the subpicosecond timescale with a modulation depth of 16% was observed. The subpicosecond decrease arises from the increase in the density of carriers, thus leading to the increase in conductivity. The optical conductivity of graphene was fitted with the Drude model and agreed with the experimental results. The photoinduced subpicosecond response reported here demonstrates that the THz response of graphene can be strongly tuned by the optical pump, which can be applied in high-performance THz modulators and ultrafast switchable THz devices.

This work was supported by the 973 Program of China (No. 2013CBA01702), the National Natural Science Foundation of China (Nos. 11474206, 91233202, 11374216, and 11404224), the Program for New Century Excellent Talents in University (NCET-12-0607), the Scientific Research Project of Beijing Education Commission (KM201310028005), the Specialized Research Fund for the Doctoral Program of Higher Education (20121108120009), and the Scientific Research Base Development Program of the Beijing Municipal Commission of Education.

- ¹K. S. Novoselov, A. K. Geim, S. V. Morozov, D. Jiang, Y. Zhang, S. V. Dubonos, I. V. Grigorieva, and A. A. Firsov, *Science* **306**, 666 (2004).
- ²Y. Zhang, Y. W. Tan, H. L. Stormer, and P. Kim, *Nature* **438**, 201 (2005).
- ³S. Kim, J. Nah, I. Jo, D. Shahrjerdi, L. Colombo, Z. Yao, E. Tutuc, and S. K. Banerjee, *Appl. Phys. Lett.* **94**, 062107 (2009).
- ⁴J. M. Dawlaty, S. Shivaraman, J. Strait, P. George, M. Chandrashekar, F. Rana, M. G. Spencer, D. Veksler, and Y. Q. Chen, *Appl. Phys. Lett.* **93**, 131905 (2008).
- ⁵K. F. Mak, Y. Wu, C. H. Lui, J. A. Misewich, and T. F. Heinz, *Phys. Rev. Lett.* **101**, 196405 (2008).
- ⁶R. R. Nair, P. Blake, A. N. Grigorenko, K. S. Novoselov, T. J. Booth, T. Stauber, N. M. R. Peres, and A. K. Geim, *Science* **320**, 1308 (2008).
- ⁷K. S. Kim, Y. Zhao, H. Jang, S. Y. Lee, J. M. Kim, K. S. Kim, J. H. Ahn, P. Kim, J. Y. Choi, and B. H. Hong, *Nature* **457**, 706 (2009).
- ⁸T. Mueller, F. Xia, and P. Avouris, *Nat. Photonics* **4**, 297 (2010).
- ⁹H. Choi, F. Borondics, D. A. Siegel, S. Y. Zhou, M. C. Martin, A. Lanzara, and R. A. Kaindl, *Appl. Phys. Lett.* **94**, 172102 (2009).
- ¹⁰S. Winnerl, M. Orlita, P. Plochocka, P. Kossacki, M. Potemski, T. Winzer, E. Malic, A. Knorr, M. Sprinkle, C. Berger, W. A. Heer, H. Schneider, and M. Helm, *Phys. Rev. Lett.* **107**, 237401 (2011).
- ¹¹N. Kakenov, T. Takan, V. A. Ozkan, O. Balci, E. O. Polat, H. Altan, and C. Kocabas, *Opt. Lett.* **40**, 1984 (2015).
- ¹²K. Yang, S. Liu, S. Arezoomandan, A. Nahata, and B. Sensale-Rodriguez, *Appl. Phys. Lett.* **105**, 093105 (2014).
- ¹³A. R. Davoyan, M. Y. Morozov, V. V. Popov, A. Satou, and T. Otsuji, *Appl. Phys. Lett.* **103**, 251102 (2013).
- ¹⁴P. Weis, J. L. Garcia-Pomar, M. Hoh, B. Reinhard, A. Brodyanski, and M. Rahm, *ACS Nano* **6**, 9118 (2012).
- ¹⁵Q. Y. Wen, W. Tian, Q. Mao, Z. Chen, W. W. Liu, Q. H. Yang, M. Sanderson, and H. W. Zhang, *Sci. Rep.* **4**, 7409 (2014).
- ¹⁶J. H. Strait, H. Wang, S. Shivaraman, V. Shields, M. Spencer, and F. Rana, *Nano Lett.* **11**, 4902 (2011).

- ¹⁷H. Wang, J. H. Strait, P. A. George, S. Shivaraman, V. B. Shields, M. Chandrashekar, J. H. wang, F. Rana, M. G. Spencer, C. S. Ruiz Vargas, and J. Park, *Appl. Phys. Lett.* **96**, 081917 (2010).
- ¹⁸S. F. Shi, T. T. Tang, B. Zeng, L. Ju, Q. Zhou, A. Zettl, and F. Wang, *Nano Lett.* **14**, 1578 (2014).
- ¹⁹A. J. Frenzel, C. H. Lui, Y. C. Shin, J. Kong, and N. Gedik, *Phys. Rev. Lett.* **113**, 056602 (2014).
- ²⁰F. Xia, T. Mueller, Y. M. Lin, A. Valdes-Garcia, and P. Avouris, *Nat. Nanotechnol.* **4**, 839 (2009).
- ²¹V. Ryzhii, M. Ryzhii, V. Mitin, and T. Otsuji, *J. Appl. Phys.* **107**, 054512 (2010).
- ²²V. I. Merkulov, D. H. Lowndes, Y. Y. Wei, G. Eres, and E. Voelkl, *Appl. Phys. Lett.* **76**, 3555 (2000).
- ²³A. E. Rider, S. Kumar, S. A. Furman, and K. K. Ostrikov, *Chem. Commun.* **48**, 2659 (2012).
- ²⁴D. H. Seo, S. Kumar, and K. Ostrikov, *J. Mater. Chem.* **21**, 16339 (2011).
- ²⁵P. Liu, Y. Wei, K. Liu, L. Liu, K. Jiang, and S. Fan, *Nano Lett.* **12**, 2391 (2012).
- ²⁶M. Z. Cai, R. A. Outlaw, S. M. Butler, and J. R. Miller, *Carbon* **50**, 5481 (2012).
- ²⁷X. Lu, G. Wang, T. Zhai, M. Yu, S. Xie, and Y. Ling, *Nano Lett.* **12**, 5376 (2012).
- ²⁸Z. Bo, W. Zhu, W. Ma, Z. Wen, X. Shuai, J. Chen, J. H. Yan, Z. H. Wang, K. F. Cen, and X. L. Feng, *Adv. Mater.* **25**, 5799 (2013).
- ²⁹H. J. Kim, Z. H. Wen, K. H. Yu, O. Mao, and J. H. Chen, *J. Mater. Chem.* **22**, 15514 (2012).
- ³⁰G. Jnawali, Y. Rao, H. G. Yan, and T. F. Heinz, *Nano Lett.* **13**, 524 (2013).
- ³¹A. J. Frenzel, C. H. Lui, W. Fang, N. L. Nair, P. K. Herring, P. Jarillo-Herrero, J. Kong, and N. Gedik, *Appl. Phys. Lett.* **102**, 113111 (2013).
- ³²Q. L. Zhou, Y. L. Shi, B. Jin, and C. L. Zhang, *Appl. Phys. Lett.* **93**, 102103 (2008).
- ³³I. Maeng, S. Lim, S. J. Chae, Y. H. Lee, H. Choi, and J. H. Son, *Nano Lett.* **12**, 551 (2012).
- ³⁴J. D. Buron, D. H. Petersen, P. Boggild, D. G. Cooke, M. Hilke, J. Sun, E. Whiteway, P. F. Nielsen, O. Hansen, A. Yurgens, and P. U. Jepsen, *Nano Lett.* **12**, 5074 (2012).
- ³⁵E. H. Hwang, S. Adam, and S. D. Sarma, *Phys. Rev. Lett.* **98**, 186806 (2007).
- ³⁶T. Ando, *Phys. Soc. Jpn.* **75**, 074716 (2006).